Electric field of Ions in solution probed by hyper-Rayleigh scattering

David P. Shelton[a)]
Department of Physics and Astronomy, University of Nevada, Las Vegas, Nevada 89154-4002, USA

(Received 11 December 2008; accepted 8 February 2009; published online 17 March 2009)

The electric field of dissolved ions accounts for the narrow spike at zero frequency shift, with the polarization signature of a polar longitudinal collective mode, in the high resolution hyper-Rayleigh light scattering (HRS) spectrum for liquid water and other polar solvents. This peak in the HRS spectrum probes both the structure factor and the fluctuation time for the ion charge density in solution. The experimental results for KCl–D_2O solutions are consistent with the Debye–Hückel charge structure factor and determine the diffusion coefficient and static local field factor.
 [DOI: 10.1063/1.3089882]

I. INTRODUCTION

The positions and motions of ions are highly correlated even in a very dilute electrolyte solution due to the long range of the Coulomb electrical interaction. The first successful theory for electrolyte solutions was proposed by Debye and Hückel,[1] and its success in accounting for the concentration dependence of phenomena such as electrical conductivity for dilute solutions of simple electrolytes is well established.[2–4] However, dilute solutions of highly charged electrolytes are still a subject of study,[5–8] and although the ion structure factors at short range are probed by neutron and x-ray scattering,[9,10] there has been no generally applicable technique which directly probes the long-range ion correlations and dynamics in bulk ionic solutions. As shown here, hyper-Rayleigh scattering (HRS) can provide such a probe.

The HRS experiment reported here measures the spectrum of the light scattered by liquid D_2O with dissolved KCl, near the second harmonic frequency of the incident laser beam, for the combination of incident and scattered light polarizations denoted as VH (where V denotes vertical linear incident-electric-field polarization and H denotes horizontal linear scattered-electric-field polarization, and the scattering plane is horizontal). A narrow spike is observed at zero frequency shift in the VH HRS spectrum but is absent from the VV and HV HRS spectra, which identifies it as due to a longitudinal polar collective mode.[11,12] This spike had been observed in the HRS spectra of several dipolar liquids, and it was at first thought to be related to ferroelectric ordering of the dipolar molecules.[13–16] This work shows that the spike is due to the electric field of dissolved ions acting on the solvent molecules.

II. THEORY

Consider the electric field of a single ion with charge Ze dissolved in a polar solvent with static dielectric constant ε_s,

$$\vec{E}(\vec{r}) = \frac{Ze}{4\pi\varepsilon_0\varepsilon_s r^2}\hat{r}. \tag{1}$$

The electric field of this ion will orient the surrounding dipolar molecules and break the local centrosymmetry of the liquid on a spatial scale large compared to the size of the molecules, inducing a macroscopic second-order nonlinear optical (NLO) susceptibility in the solvent. An incident light wave at frequency ν polarized $\parallel$ or $\perp$ to the ion field $E^{(0)}$ will induce molecular dipoles oscillating at frequency 2ν polarized $\parallel$ to $E^{(0)}$,[17]

$$\mu^{(2\nu)} = \frac{1}{4}\left[\gamma_{\parallel,\perp} + \frac{\mu^{(0)}\beta_{\parallel,\perp}}{3k_BT}\right](f(\nu)E^{(\nu)}_{\parallel,\perp})^2 f(0)E^{(0)}, \tag{2}$$

where $\mu^{(0)}$ is the permanent dipole moment of a solvent molecule, k_B is the Boltzmann constant, $f(\nu)=(n^2+2)/3$ is the Lorentz local field factor at optical frequency ν, n is the solvent refractive index,

$$f(0) = \frac{\varepsilon_s(\varepsilon_\infty + 2)}{\varepsilon_\infty + 2\varepsilon_s} \tag{3}$$

is the Onsager static local field factor,[18] and ε_∞ is the infinite frequency permittivity.[19] Equation (2) will typically be valid for $r \geq 1$ nm where the field of the ion is weak enough so that $\mu^{(0)}E^{(0)}/3k_BT \ll 1$. The vector components of the molecular first hyperpolarizability $\beta(-2\nu;\nu,\nu)$ and the scalar components of the second hyperpolarizability $\gamma(-2\nu;\nu,\nu,0)$ appearing in Eq. (2) are given by sums over molecule frame tensor components,[17]

$$\beta_\parallel = \frac{1}{5}\sum_\xi(\beta_{z\xi\xi} + 2\beta_{\xi\xi z}), \tag{4}$$

$$\beta_\perp = \frac{1}{5}\sum_\xi(2\beta_{z\xi\xi} - \beta_{\xi\xi z}), \tag{5}$$

$$\gamma_\parallel = \frac{1}{15}\sum_{\xi\eta}(\gamma_{\xi\eta\eta\xi} + 2\gamma_{\xi\xi\eta\eta}), \tag{6}$$

a)Electronic mail: shelton@physics.unlv.edu.

$$\gamma_{\perp} = \frac{1}{15}\sum_{\xi\eta}(2\gamma_{\xi\eta\eta\xi} - \gamma_{\xi\xi\eta\eta}), \tag{7}$$

where the direction of $\mu^{(0)}$ is chosen as the direction of the molecular z axis. When the tensor components are invariant under all permutations of the indices (Kleinman symmetry), these expressions simplify to

$$\beta_{\parallel} = 3\beta_{\perp} = \frac{3}{5}\sum_{\xi}\beta_{z\xi\xi}, \tag{8}$$

$$\gamma_{\parallel} = 3\gamma_{\perp} = \frac{1}{5}\sum_{\xi\eta}\gamma_{\xi\xi\eta\eta}. \tag{9}$$

Kleinman symmetry is exact in the static limit and is often a good approximation at optical frequencies. The oscillating dipoles given by Eq. (2) will radiate second harmonic light waves.

The HRS wave observed in a particular direction is due to the Fourier component of the spatially varying material nonlinear susceptibility that satisfies the wavevector matching (constructive interference) condition $\vec{k}=2\vec{k}_i-\vec{k}_f$, where i and f label the initial and final photon wavevectors. The macroscopic spatial variation in the NLO susceptibility is due to the spatial variation in ion field $E^{(0)}$ given by Eq. (1). Decomposing this field into plane waves, one sees that the transverse polarized plane wave Fourier components vanish by symmetry. The only nonvanishing components of this field are the longitudinally polarized Fourier sine components, with amplitudes

$$A(\vec{k}) = \frac{Ze}{\varepsilon_0\varepsilon_s}\frac{1}{k}. \tag{10}$$

The VH HRS intensity at 90° scattering angle due to the longitudinal polar mode induced by a single ion in solution is

$$I \propto \left[\rho_s\frac{1}{\sqrt{2}}\left(\gamma_{\perp} + \frac{\mu^{(0)}\beta_{\perp}}{3k_BT}\right)A(\vec{k})f(0)\right]^2, \tag{11}$$

where ρ_s is the number density of solvent molecules and $1/\sqrt{2}$ is the projection factor which arises since $\vec{k}$ is at 45° to the observation direction.[11,12]

For comparison, the VH HRS intensity due to randomly oriented solvent molecules is[20,21]

$$I \propto V\rho_s\langle\beta^2_{XZZ}\rangle, \tag{12}$$

where V is the sample volume and the constant of proportionality is the same as in Eq. (11). The mean square laboratory frame hyperpolarizability $\langle\beta^2_{XZZ}\rangle$ is the sum of first rank (vector) and third rank (octupolar) irreducible spherical tensor contributions, and also contributions of mixed symmetry which vanish when Kleinman symmetry holds[21]

$$\langle\beta^2_{XZZ}\rangle = \frac{1}{45}|\beta^{(1)}|^2 + \frac{4}{105}|\beta^{(3)}|^2 + \frac{2}{45}[\beta^{2(\mathrm{ms})}]. \tag{13}$$

Expressions in terms of molecule frame Cartesian components for molecules of C_{2v} symmetry are[20–22]

$$|\beta^{(1)}|^2 = \tfrac{3}{5}(A+B+C)^2 = \tfrac{5}{3}\beta^2_{\parallel}, \tag{14}$$

$$|\beta^{(3)}|^2 = \tfrac{1}{10}(2A-3B-3C)^2 + \tfrac{3}{2}(B-C)^2, \tag{15}$$

$$[\beta^{2(\mathrm{ms})}] = -(A+B+C)(D+E) + \tfrac{87}{105}(D+E)^2 + \tfrac{1}{2}(D-E)^2, \tag{16}$$

where $A=\beta_{zzz}$, $B=(2\beta_{yyz}+\beta_{zyy})/3$, $C=(2\beta_{xxz}+\beta_{zxx})/3$, $D=(\beta_{yyz}-\beta_{zyy})$, and $E=(\beta_{xxz}-\beta_{zxx})$. In the case that β_{zzz} is the only nonvanishing tensor component $\beta^2_{\perp}/\langle\beta^2_{XZZ}\rangle=7/5$, while in the case that Kleinman symmetry holds and the octupolar contribution vanishes, one has $\beta^2_{\perp}/\langle\beta^2_{XZZ}\rangle=3$.

In a sufficiently dilute solution the ion positions and the relative phases of the scattered waves due to the individual ions are random, so the total scattered intensity is the incoherent sum of the single ion contributions. For a symmetric electrolyte the intensity given by Eq. (11) is multiplied by $V(\rho_+ + \rho_-)=2V\rho$, where ρ_+ and ρ_- are the number densities of + and − ions, respectively. In a more concentrated solution the ion positions are correlated, and the Debye–Hückel theory gives the charge structure factor

$$S(\vec{k}) = \frac{k^2}{k^2 + K_D^2}, \tag{17}$$

where

$$K_D^2 = \frac{2\rho Z^2e^2}{\varepsilon_0\varepsilon_s k_BT} \tag{18}$$

is the Debye–Hückel screening parameter.[23,24] Combining Eqs. (10)–(12) and (17) gives an expression for the ratio of the VH HRS spike intensity (S) to the background intensity from the randomly oriented solvent molecules (B),

$$S/B = \frac{\rho\rho_s Z^2e^2}{k^2+K_D^2}\left[\frac{f(0)}{\varepsilon_0\varepsilon_s}\right]^2\frac{[\gamma_{\perp} + \mu^{(0)}\beta_{\perp}/3k_BT]^2}{\langle\beta^2_{XZZ}\rangle}. \tag{19}$$

Ignoring the ρ dependence of ρ_s, ε_s, and $f(0)$, this expression may be written in the form

$$S/B = (S/B)_{\infty}\frac{\rho/\rho_D}{1+\rho/\rho_D}, \tag{20}$$

where

$$\rho_D = \frac{k^2\varepsilon_0\varepsilon_s k_BT}{2Z^2e^2} \tag{21}$$

is the electrolyte density for which $K_D^2=k^2$, and

$$(S/B)_{\infty} = \frac{\rho_s f(0)^2 k_BT}{2\varepsilon_0\varepsilon_s}\frac{[\gamma_{\perp} + \mu^{(0)}\beta_{\perp}/3k_BT]^2}{\langle\beta^2_{XZZ}\rangle} \tag{22}$$

is the limiting value of S/B at high ρ.

Charge density fluctuations cause fluctuations in the scattered light, and the fluctuation relaxation time scale and consequent spectral broadening are governed by diffusion of the ions. For a symmetric electrolyte with ion diffusion coefficients $D_+=D_-=D$, this exponential relaxation results in a Lorentzian spectrum (the spike) with linewidth $\nu_S(k,\rho)$ given by[23]

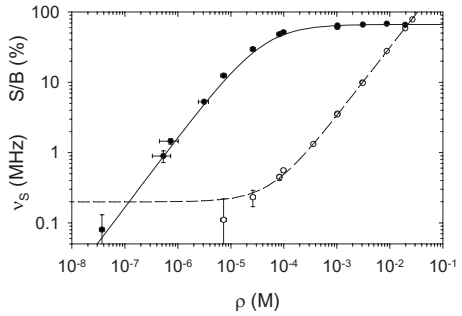

FIG. 1. VH HRS measurements for KCl–D_2O solutions at 25.0 °C plotted vs electrolyte molar concentration ρ. The data for S/B and ν_S are shown by filled and open circles, respectively. Some error bars are smaller than the plotted symbols. The solid curve is the fit of Eq. (20) to the spike intensity S/B, while the dashed curve is the fit of Eq. (23) to the spectral width ν_S.

$$\nu_S(k,\rho) = \frac{k^2 D}{2\pi}\left[2 + y - \frac{1+y}{2+y}\right], \tag{23}$$

where

$$y = (K_D/k)^2 = \rho/\rho_D. \tag{24}$$

D for the ions, as experimentally determined from the equivalent conductivity of ionic solutions using the Nernst–Einstein equation, has the limiting value D_0 at $\rho=0$ and is a decreasing function of $\rho^{1/2}$.[3,4]

III. EXPERIMENT

The experimental apparatus and methods to measure the high resolution VH HRS spectrum are similar to those previously described.[16,25] D_2O rather than H_2O was used to reduce undesired thermal lensing due to absorption of the 1064 nm laser beam in the sample; isotopic purity of all samples was >99% D. Solutions of KCl (>99% purity) in D_2O at concentrations above $\rho=0.3$ mM KCl were prepared by weight as in previous work, while at lower concentration ρ was determined from the sample conductivity.[26–28] Deionized and dust-free D_2O (66 MΩ cm at 25.0 °C)[26,28] was prepared using a recirculating loop containing a mixed bed ion exchange resin, a 0.2 μm particle filter, conductivity sensors, and the sample cuvette.

The high resolution VH HRS spectrum consists of a narrow spike riding on a broad, flat background, from which one obtains the ratio of integrated intensities for the spike and the background (S/B), and the Lorentzian spectral width (ν_S) for the spike.[16,25] The results of the VH HRS measurements for KCl solutions are shown in Fig. 1. The vertical error bars represent the uncertainties in S/B and ν_S due to photon counting statistics (about 2% on the data points down to $\rho=7$ μM for S/B or 0.3 mM for ν_S) and other factors (2%). Not included in the vertical error bars are potential errors due to dust which is sometimes present in a sample (the effect of dust is to increase S/B and decrease ν_S). The variable ρ on the horizontal axis is half the total ion concentration in the sample. The ionic composition of the samples varies, and the ions in the 37 nM sample are D^+ and OD^- from dissociation of the D_2O. In the range of 0.5–3 μM, the ions are K^+ and Cl^- deliberately added to the sample and D^+ and DCO_3^- from dissolved atmospheric CO_2 introduced through air leaks in the apparatus (the horizontal error bars show the full range of ρ consistent with the measured conductivity). Above 3 μM the ions are K^+ and Cl^-. The horizontal error bars include 10% uncertainty from the conductivity sensor calibration for points below 0.3 mM and represent 2% sample composition uncertainty for points above 0.3 mM.

Figure 1 shows the curves obtained by fitting Eq. (20) to the S/B data and Eq. (23) to the ν_S data. The ρ dependence of D in Eq. (23) was determined using the measured equivalent conductivity Λ for KCl dissolved in D_2O and the relation $D/D_0=\Lambda/\Lambda_0$.[27] The fit to the data is good except for a small discrepancy for S/B in the crossover region. This could be due to the conductivity sensor calibration or a small excess intensity from dust for those points. The results for the three adjustable parameters in the fits are $(S/B)_\infty = 0.667 \pm 0.008$ (spike intensity limit), $k^2 D_0/2\pi\rho_D = 3310 \pm 43$ MHz/M (slope of the spectral width curve), and $\rho_D = 40 \pm 8$ μM (crossover concentration).

IV. DISCUSSION

The slope parameter in the spectral width curve may be expressed using Eqs. (21), (23), and (24) as $k^2 D_0/2\pi\rho_D = D_0 Z^2 e^2/\pi\varepsilon_0\varepsilon_s k_B T = 2864$ MHz/M, evaluated using the material parameter values $\varepsilon_s=78.08$ for D_2O at 25.0 °C,[29] and $D_0 = 1.656\times10^{-9}$ m^2 s^{-1} for K^+ and Cl^- in D_2O at 25.0 °C obtained from conductivity measurements.[27] Evaluation of the crossover concentration ρ_D given by Eq. (21) also requires the experimental scattering wavevector k. Assuming $n_{532}=1.335$ and $n_{1064}=1.323$,[30–32] the values $2\pi/k = 283$ nm and $\rho_D = 45.3$ μM are obtained for 90° scattering of the 1064 nm laser beam. The experimentally determined crossover parameter is 12% lower than the theoretical prediction, but agrees to within the experimental uncertainty. The experimentally determined slope parameter is 16% ± 1.5% higher than the theoretical prediction, which suggests that a different D_0 is being measured. The theoretical prediction was based on the self-diffusion coefficient obtained from conductivity measurements, but the relaxation of charge fluctuations probed in this experiment may instead be related to the mutual diffusion coefficient. One recent calculation finds that the ratio of mutual and self-diffusion coefficients for water molecules in KCl solutions is $D_m/D_s = 1.13$,[33] which is consistent with the observed discrepancy. However, a different calculation for diffusion of KCl in water indicates that $D_m/D_s < 1.02$ over the concentration range of this experiment,[34] so the issue needs further investigation.

The expression for the limiting spike intensity ratio $(S/B)_\infty$ given by Eq. (22) is evaluated using $\rho_s=55.1$ M,[27] $\varepsilon_\infty=4.49$,[35] and calculated values for the dipole moment[36] and hyperpolarizabilities[37] for D_2O molecules in the liquid: $\mu^{(0)}=2.95$ D $=9.84\times10^{-30}$ C m, $\beta_{zzz}=31.6$ a.u., $\beta_{zyy}=10.9$ a.u., $\beta_{zxx}=5.7$ a.u., $\beta_\perp=9.64$ a.u. $=3.09\times10^{-52}$ C^3 m^3 J^{-2}, and $\gamma_\perp=892$ a.u. $=5.56\times10^{-62}$ C^4 m^4 J^{-3}. The γ contribution is relatively small but not negligible, $3k_BT\gamma_\perp/\mu^{(0)}\beta_\perp=0.226$, and the vector part of β is dominant, giving $\beta_\perp^2/\langle\beta_{XZZ}^2\rangle=2.80$. Although β increases 200% going from gas phase to liquid, the ratio

$\beta_{\perp}^2/\langle\beta_{XZZ}^2\rangle$ only increases 4%.[37] However, calculated hyperpolarizabilities are very sensitive to the basis set and correlation treatment, and consideration of other calculations for the water molecule suggests that the β ratio given above may be too large by about 11%. The ratios calculated from the static gas phase results from Refs. 38 and 39 are 8% smaller than corresponding gas phase result from Ref. 37. The ratio also decreases a further 3% when vibrational hyperpolarizability terms and frequency dispersion are included.[22,39] Assuming that the result from Ref. 37 for liquid water is an 11% overestimate gives the revised estimate $\beta_{\perp}^2/\langle\beta_{XZZ}^2\rangle = 2.52$ for liquid D_2O. Using the local field factor $f(0) = 3.15$ given by Eq. (3), one obtains the predicted value $(S/B)_{\infty} = 2.36$ which is much higher than the fitted value of 0.667.

However, the background intensity measured in the experiment includes the entire HRS spectrum in the 60 cm^{-1} instrument bandpass, whereas the assumed background in Eq. (22), expressed through the factor $\langle\beta_{XZZ}^2\rangle$, is just the pure rotational HRS spectrum. The pure rotational HRS spectrum of water is a 1 cm^{-1} wide peak, which is surrounded by the broad spectral wings of the collision-induced spectrum due to the rapid molecular hyperpolarizability modulation during intermolecular collisions. Previous low resolution HRS spectral measurements for D_2O show that the central 1 cm^{-1} wide pure rotation peak contributes just $54 \pm 6\%$ of the VH HRS integrated intensity in a 60 cm^{-1} passband.[22] Therefore, the experimental value that should be compared with the result from Eq. (22) is $(S/B)_{\infty} = 0.667/0.54 = 1.23 \pm 0.14$. This is still 1.92 times smaller than the predicted value of 2.36.

Possible sources for the discrepancy are errors in the values for $\mu^{(0)}$, β, γ, or $f(0)$ in Eq. (22). The effective molecular property values in the liquid were obtained using *ab initio* and molecular dynamics calculations which include the detailed structure of the molecules and the liquid, while the Onsager local field factor is based on a continuum model. If the local field factor is the problem, then one can obtain agreement between theory and experiment for $(S/B)_{\infty}$ by reducing $f(0)$ from 3.15 to 2.27. This is consistent with recent molecular dynamics simulations which find that the usual Onsager local field factor given by Eq. (3) overestimates the actual local field factor.[40,41] So far there has not been a satisfactory method to experimentally determine the static local field factor, but the present experiment has the potential to measure it fairly directly. This is because the electric-field-induced second harmonic signal sensitive to $f(0)$ in this experiment is calibrated by a second harmonic signal independent of $f(0)$ but due to the same property of the same molecules in the same environment measured at the same time.

In summary, electric-field-induced second harmonic generation occurs in ionic solutions due to the electric fields of the dissolved ions. The resulting scattered light appears as a narrow peak in the VH HRS spectrum. The intensity and width of this peak carry information about the long-range ion correlations and dynamics and hold promise as a means to experimentally measure the static local field factor in polar liquids. Based on the present results it is most probable that the VH spike observed in water,[22,42] acetonitrile,[13] nitromethane,[14,15] and nitrobenzene,[16,25] previously attributed to ferroelectric ordering of the dipoles, is actually due to ionic contamination. Ionic salts easily dissolve and dissociate in such strongly polar solvents, and ion concentrations of just a few micromolars are sufficient to account for the observations. Measurements on de-ionized solvents would settle the matter.

[1] P. Debye and E. Hückel, Phys. Z. **24**, 185 (1923).
[2] R. A. Robinson and R. H. Stokes, *Electrolyte Solutions*, 2nd ed. (Butterworths, London, 1968).
[3] J. O'M. Bockris and A. K. N. Reddy, *Modern Electrochemistry*, 2nd ed. (Plenum, New York, 1998), Vol. 1.
[4] W. R. Fawcett, *Liquids, Solutions, and Interfaces* (Oxford University Press, New York, 2004).
[5] T. T. Nguyen, A. Yu. Grosberg, and B. I. Shklovskii, Phys. Rev. Lett. **85**, 1568 (2000).
[6] E. Trizac, L. Bocquet, and M. Aubouy, Phys. Rev. Lett. **89**, 248301 (2002).
[7] J. C. Butler, T. Angelini, J. X. Tang, and G. C. L. Wong, Phys. Rev. Lett. **91**, 028301 (2003).
[8] T. S. Lo, B. Khusid, and J. Koplik, Phys. Rev. Lett. **100**, 128301 (2008).
[9] J. E. Enderby and G. W. Neilson, Rep. Prog. Phys. **44**, 593 (1981).
[10] H. E. Fischer, A. C. Barnes, and P. S. Salmon, Rep. Prog. Phys. **69**, 233 (2006).
[11] V. N. Denisov, B. N. Mavrin, and V. B. Podobedov, Phys. Rep. **151**, 1 (1987).
[12] D. P. Shelton, J. Opt. Soc. Am. B **17**, 2032 (2000).
[13] D. P. Shelton, J. Chem. Phys. **123**, 084502 (2005).
[14] D. P. Shelton, J. Chem. Phys. **123**, 111103 (2005).
[15] D. P. Shelton, J. Chem. Phys. **124**, 124509 (2006).
[16] D. P. Shelton and Z. Quine, J. Chem. Phys. **127**, 204503 (2007).
[17] D. P. Shelton and J. E. Rice, Chem. Rev. (Washington, D.C.) **94**, 3 (1994).
[18] D. M. Burland, R. D. Miller, and C. A. Walsh, Chem. Rev. (Washington, D.C.) **94**, 31 (1994).
[19] J. Barthel and R. Buchner, Pure Appl. Chem. **63**, 1473 (1991).
[20] R. Bersohn, Y.-H. Pao, and H. L. Frisch, J. Chem. Phys. **45**, 3184 (1966).
[21] P. D. Maker, Phys. Rev. A **1**, 923 (1970).
[22] D. P. Shelton, J. Chem. Phys. **117**, 9374 (2002); **121**, 3349 (2004).
[23] B. J. Berne and R. Pecora, *Dynamic Light Scattering* (Wiley, New York, 1976).
[24] J.-L. Barrat and J.-P. Hansen, *Basic Concepts for Simple and Complex Liquids* (Cambridge University Press, New York, 2003).
[25] D. P. Shelton, J. Chem. Phys. **129**, 134501 (2008).
[26] *CRC Handbook of Chemistry and Physics*, 68th ed., edited by R. C. Weast (CRC, Boca Raton, 1987).
[27] M. Nakahara, M. Zenke, M. Ueno, and K. Shimizu, J. Chem. Phys. **83**, 280 (1985).
[28] H. Weingartner and C. A. Chatzidimitriou-Dreismann, Nature (London) **346**, 548 (1990).
[29] K. R. Srinivasan and R. L. Kay, J. Chem. Phys. **60**, 3645 (1974).
[30] A. H. Harvey, J. S. Gallagher, and J. M. H. L. Sengers, J. Phys. Chem. Ref. Data **27**, 761 (1998).
[31] B. Richerzhagen, Appl. Opt. **35**, 1650 (1996).
[32] J. E. Bertie, M. K. Ahmed, and H. H. Eysel, J. Phys. Chem. **93**, 2210 (1989).
[33] A. Chandra, Phys. Rev. Lett. **85**, 768 (2000).
[34] R. Gupta and A. Chandra, J. Chem. Phys. **128**, 184506 (2008).
[35] J. Barthel, K. Bachhuber, R. Buchner, and H. Hetzenauer, Chem. Phys. Lett. **165**, 369 (1990).
[36] A. V. Gubskaya and P. G. Kusalik, J. Chem. Phys. **117**, 5290 (2002).
[37] A. V. Gubskaya and P. G. Kusalik, Mol. Phys. **99**, 1107 (2001).
[38] G. Maroulis, Chem. Phys. Lett. **289**, 403 (1998).
[39] D. Spelsberg and W. Meyer, J. Chem. Phys. **108**, 1532 (1998).
[40] Y. Tu, Y. Luo, and H. Agren, J. Phys. Chem. B **110**, 8971 (2006).
[41] H. Reis, M. G. Papadopoulos, and A. Grzybowski, J. Phys. Chem. **110**, 18537 (2006).
[42] D. P. Shelton, Phys. Rev. B **72**, 020201(R) (2005).